

Modeling and Static Analysis of a Three-Rigid-Link Object for Nonprehensile Manipulation Planning

Omar Mehrez¹, Zakarya Zyada², Member IEEE, Hossam S. Abbas³, Member IEEE and Ahmed Abo-Ismail⁴

^{1,4}*Mechatronics and Robotics Eng. Dept., Egypt-Japan University of Science and Technology, Alexandria, Egypt*

²*Adjunct Professor at Mechatronics and Robotics Eng. Dept., Egypt-Japan University of Science and Technology Mechanical Power Eng. Dept., Tanta University, Tanta, Egypt*

³*Adjunct Professor at Mechatronics and Robotics Eng. Dept., Egypt-Japan University of Science and Technology Electrical Eng. Dept., Assiut University, Assiut, Egypt*

omar.mehrez@ejust.edu.eg, zzyada@f-eng.tanta.edu.eg, hossam.abbas@ejust.edu.eg, aboismail@ejust.edu.eg

Abstract – This work presents the dynamic modeling and the static analysis of a three rigid link object manipulated by two cooperative arms in a plane. Such analysis is required as a step prior to the nonprehensile manipulation planning of the object. The system is configured in a way such that one of the two robot arms is in contact with two links of the object, while the other arm is in contact with the third link. The purpose of the static analysis is to obtain the interaction forces as well as their locations between the object links and the arms required to hold the object for a specified configuration. The dynamic model of the system is introduced, and the static analysis considering both the frictionless and frictional contact cases between the arms and the object links is deduced. The effect of changing the direction of the static frictional forces at multi contact points is introduced.

Nonprehensile manipulation, multi-link object manipulation, cooperative arms, static analysis.

I. INTRODUCTION

Nowadays the demand for human interactive robots to help caregivers on site is increasing. The task of transferring a patient from the bed to a wheelchair is the heaviest one in nursing care [1]. The use of the human type arms method is the most advantageous one for such task. An example is the robot developed by RIKEN-TRI collaboration center, RIBA, which uses its whole arms in human transfer, [2]. In such application the goal is to manipulate a multi-link heavy object using whole arm manipulation. As a step towards the most complicated task of the human manipulation this work is proposed. This study presents the dynamic modeling and the static analysis of a three-rigid link object manipulated by two robot arms in a two dimensional space, see Fig. 1.

Whole arm manipulation lies under the taxonomy of nonprehensile manipulation (without a form or force-closure) [3]. The whole arm manipulation utilizes the whole surface of the arms, using low degree of freedom robots, rather than the end effectors to perform the grasp. This is very helpful in dealing with large and/or heavy objects [4], [5]. By not grasping, the robot can use gravitational, centrifugal, and Coriolis forces as virtual motors to control more degrees of freedom of the part. This has the advantages of reducing the complexity of the arm and increasing the workspace dimensionality, but at the expense of increasing the complexity of planning and control. Many applications for manipulating one degree of freedom (1-DOF) object can be

found in the literature. As an example, the dynamic manipulation for throwing and catching a disc using two planar manipulators is presented [6]. In [7] a motion planning of a planner robot to throw an object in the horizontal plane is performed. An interesting mechanism inspired from the handling of a pizza peel is done in [8].

Regarding the problem of manipulating a multi-link object using one or more than one manipulator, not so much work is found in the literature. An earlier study for manipulating a multi-link object using two cooperative robot arms is found in [9], in which the basic task requirements, conditions and difficulties are described. A more mature study has been extended to deal with the manipulation of a two link rigid object constrained by two cooperative robot arms [10], [11], and [12]. A dynamic model of the system has been derived, static analysis has been considered and a controller for lifting up the object in a plane has been designed. The object's behaviors were considered with and without friction contacts with the arms.

Motivated by the application of lifting a human, this work is presented. It produces the first step in this direction. We propose a three-rigid link object manipulated by a two robot arms in a two dimensional space. Two links are always kept in contact with one arm, while the third link is in contact with the other arm, see Fig. 1. This configuration is more realistic to a lifted human rather than the one considered in [11], [12]. Here, the dynamic model is derived, and the static analysis of the system is performed. The static analysis means finding the positions of the arms required to keep the object statically balanced for all configurations of the object. This is carried out when no friction is considered between the arms and the object links. The study is extended to include and explore the effect of the static friction on the static analysis problem. We just considered here studying the effect of changing the direction of the static friction forces.

The paper is organized as follows: the dynamic model that represents a three rigid link object manipulated by a two cooperative arms in a plane is derived in section II. The static analysis in frictionless contact between the object and the arms is given in section III. Section IV presents the effect of considering the static friction between the object and the arms on the analysis problem. Simulation results are given in section V. Conclusions and recommendations for future work are presented in section VI.

II. SYSTEM DYNAMICS

In this section, system description, a dynamic model of the system, kinematic constraints, and visco-elastic model at a contact are presented.

A. System Description

Figure 1 illustrates the schematic diagram of the system. The object is represented by three rigid links (link-1, link-2, and link-3) connected by two passive joints: the knee and the hub joints. The angular positions of the links are given by θ_1 , θ_2 , and θ_3 respectively, see fig. 1. The position of the knee joint (x, y) is referred to the world coordinate frame Σ_o . The position of the hub joint is related to that of the knee one in terms of the length of link-2, L_2 , and its angle θ_2 by the equation:

$$x_h = x + L_2 \cos \theta_2 \quad (1a)$$

$$y_h = y + L_2 \sin \theta_2 \quad (1b)$$

The position of either the knee or the hub joint along with the angular positions of the three links complete the definition of the position and orientation of the object relative to Σ_o . The masses and mass moment of inertia of the links are denoted by m_1 and J_1 , m_2 and J_2 , m_3 and J_3 for link-1, link-2, and link-3 respectively. The distance from the knee joint to the center of gravities of link-1, 2 are denoted by L_1 , L_{2k} respectively, and the distance from the hub joint to the center of gravity of link-3 is indicated by L_3 . The object is held by two arms of radius r . The position of each arm relative to Σ_o is given as (x_{A_j}, y_{A_j}) , where $j = 1, 2$. Arm-1 is in contact with link-1 with interaction forces F_1 of distance l_1 and F_2 of distance l_2 from the knee joint respectively, whereas arm-2 is in contact with link-3 only with an interaction force F_3 of distance l_3 from the hub joint. The interaction force is decomposed into two components: the normal and the tangential forces F_N and F_T , respectively.

The following assumptions are considered:

- 1) The object links are rigid
- 2) The contact between the object links and the arms is soft.
- 3) The contact between the arms and the object links in a plane is a line.
- 4) The tangential friction forces F_{iT} ($i = 1, 2, 3$) are constant at any point throughout the line of contact, and in turn the resultant interaction force F_i is affecting at the middle of the line of contact.

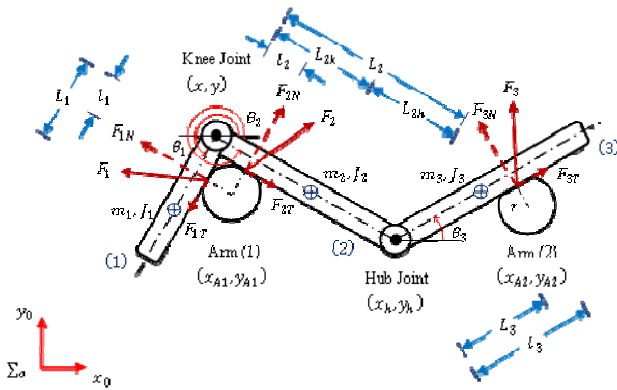


Fig.1 Schematic diagram of the system

B. Dynamic Modeling

The state vector which is required to completely define the object pose can be defined by:

$$q = [x \ y \ \theta_1 \ \theta_2 \ \theta_3]^T \quad (2)$$

The dynamic model of the system is obtained using the Lagrange method in the direction of the state variables, then putting in the form:

$$M(q)\ddot{q} + C(q, \dot{q})\dot{q} + G(q) = B(q, l)u \quad (3)$$

The terms $M(q)$, $C(q, \dot{q})$, and $G(q)$ are given in (9) in next page. $B(q, l)$ and u are defined by:

$$B(q, l) = \begin{bmatrix} 1 & 0 & 1 & 0 & 1 & 0 \\ 0 & 1 & 0 & 1 & 0 & 1 \\ -l_1 \sin \theta_1 & l_1 \cos \theta_1 & 0 & 0 & 0 & 0 \\ 0 & 0 & -l_2 \sin \theta_2 & l_2 \cos \theta_2 & 0 & 0 \\ 0 & 0 & 0 & 0 & -l_3 \sin \theta_3 & l_3 \cos \theta_3 \end{bmatrix}, \quad (4)$$

$$u = [u_1^T \ u_2^T \ u_3^T]^T = [F_{1x} \ F_{1y} \ F_{2x} \ F_{2y} \ F_{3x} \ F_{3y}]^T \quad (5)$$

with:

$$\begin{aligned} u_1 &= \begin{bmatrix} \sin \theta_1 & \cos \theta_1 \end{bmatrix} \begin{bmatrix} F_{1N} \\ F_{1T} \end{bmatrix} = \begin{bmatrix} F_{1x} \\ F_{1y} \end{bmatrix} \\ u_2 &= \begin{bmatrix} -\sin \theta_2 & \cos \theta_2 \end{bmatrix} \begin{bmatrix} F_{2N} \\ F_{2T} \end{bmatrix} = \begin{bmatrix} F_{2x} \\ F_{2y} \end{bmatrix} \\ u_3 &= \begin{bmatrix} -\sin \theta_3 & \cos \theta_3 \end{bmatrix} \begin{bmatrix} F_{3N} \\ F_{3T} \end{bmatrix} = \begin{bmatrix} F_{3x} \\ F_{3y} \end{bmatrix} \end{aligned} \quad (6)$$

The distances l_1 , l_2 , and l_3 are given as a function of the positions of the two robot arms by:

$$\left. \begin{aligned} l_1 &= (y_{A1} - y) \sin \theta_1 + (x_{A1} - x) \cos \theta_1 \\ l_2 &= (y_{A1} - y) \sin \theta_2 + (x_{A1} - x) \cos \theta_2 \\ l_3 &= (y_{A2} - y_h) \sin \theta_3 + (x_{A2} - x_h) \cos \theta_3 \end{aligned} \right\} \quad (7)$$

C. Contact Model

The contact between the arm and the object can be modeled using the visco-elastic model [11], see fig. 2, as:

$$F_{iN} = \begin{cases} k_i \delta_i + d_i \dot{\delta}_i, & \text{for } \delta \geq 0 \\ 0, & \text{for } \delta < 0 \end{cases} \quad (8)$$

where, F_{iN} is the normal component of the interaction force, δ_i is the radial deformation of the arm in the direction of the normal force, $\dot{\delta}_i$ is its rate of change, k_i , d_i denote the spring constant, and damping coefficient respectively, $i = 1, 2, 3$.

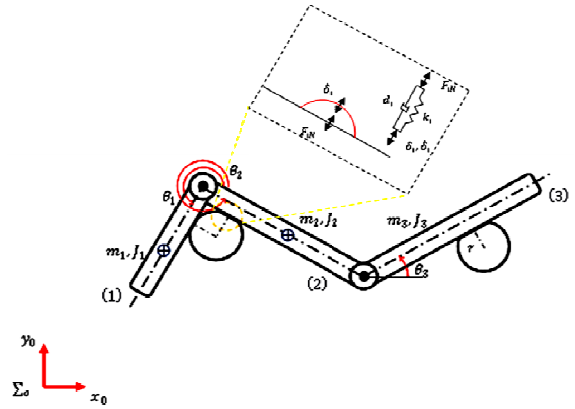


Fig. 2. Visco-elastic model at the contact

$$M(q) = \begin{bmatrix} (m_1 + m_2 + m_3) & 0 & -(m_1 L_1) \sin \theta_1 & -(m_2 L_{2K} + m_3 L_2) \sin \theta_2 & -(m_3 L_3) \sin \theta_3 \\ 0 & (m_1 + m_2 + m_3) & (m_1 L_1) \cos \theta_1 & (m_2 L_{2K} + m_3 L_2) \cos \theta_2 & (m_3 L_3) \cos \theta_3 \\ -(m_1 L_1) \sin \theta_1 & (m_1 L_1) \cos \theta_1 & (J_1 + m_1 L_1^2) & 0 & 0 \\ -(m_2 L_{2K} + m_3 L_2) \sin \theta_2 & (m_2 L_{2K} + m_3 L_2) \cos \theta_2 & 0 & (J_2 + m_2 L_{2K}^2 + m_3 L_2^2) & (m_3 L_2 L_3) \cos(\theta_2 - \theta_3) \\ -(m_3 L_3) \sin \theta_3 & (m_3 L_3) \cos \theta_3 & 0 & (m_3 L_2 L_3) \cos(\theta_2 - \theta_3) & (J_3 + m_3 L_3^2) \end{bmatrix},$$

$$C(q, \dot{q}) = \begin{bmatrix} 0 & 0 & -(m_1 L_1) \dot{\theta}_1 \cos \theta_1 & -(m_2 L_{2K} + m_3 L_2) \dot{\theta}_2 \cos \theta_2 & -(m_3 L_3) \dot{\theta}_3 \cos \theta_3 \\ 0 & 0 & -(m_1 L_1) \dot{\theta}_1 \sin \theta_1 & -(m_2 L_{2K} + m_3 L_2) \dot{\theta}_2 \sin \theta_2 & -(m_3 L_3) \dot{\theta}_3 \sin \theta_3 \\ 0 & 0 & 0 & 0 & 0 \\ 0 & 0 & 0 & 0 & (m_3 L_2 L_3) \dot{\theta}_3 \sin(\theta_2 - \theta_3) \\ 0 & 0 & 0 & -(m_3 L_2 L_3) \dot{\theta}_2 \sin(\theta_2 - \theta_3) & 0 \end{bmatrix},$$

$$G(q) = [0 \quad (m_1 + m_2 + m_3)g \quad (m_1 L_1)g \cos \theta_1 \quad (m_2 L_{2K} + m_3 L_2)g \cos \theta_2 \quad (m_3 L_3)g \cos \theta_3]^T$$

D. Kinematic Constraint of Link-1 and Link-2

Since arm-1 is kept in contact with both link-1 and link-2, there is a kinematic constraint in terms of the angular positions of links-1, 2, see fig. 3, defined by:

$$\theta_2 - \theta_1 = \theta_{01} + \theta_{02} \quad (10)$$

where $\theta_{01} + \theta_{02}$ is the angle between the two links, the following two nonlinear relations can be obtained:

$$\begin{aligned} l_1^2 + (r - c_1/l_1)^2 &= l_2^2 + (r - c_2/l_2)^2 \\ \frac{l_2(r - c_1/l_1) + l_1(r - c_2/l_2)}{l_1 l_2 - (r - c_1/l_1)(r - c_2/l_2)} &= \tan(\theta_2 - \theta_1) \end{aligned} \quad (11)$$

where:

$$c_1 = \frac{-m_1 * L_1 * g * \cos \theta_1}{k_i}, c_2 = \frac{(m_2 * L_{2K} + m_3 * L_2) * g * \cos \theta_2}{k_i}$$

where k_i denotes the spring constant defined in (8).

III. STATIC ANALYSIS

For the problem of the nonprehensile manipulation, not only the interaction forces between the object and the arm are interested to keep the object grasped, but also their locations. The purpose of the static analysis is to determine the values of such interaction forces and their locations for every pose of the object. Next, we discuss when frictionless contacts between the arms and the object is considered; this means that $F_i = F_{iN}$, and $F_{iT} = 0$.

In this work, the ranges of change of the angles are restricted as:

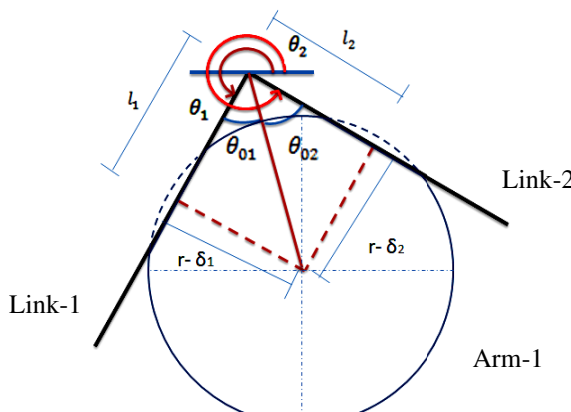


Fig. 3. Kinematic constraint of link (1) and link (2)

$$\left. \begin{array}{l} 180^\circ \leq \theta_1 \leq 270^\circ \\ 270^\circ \leq \theta_2 \leq 360^\circ \\ 0^\circ \leq \theta_3 \leq 90^\circ \end{array} \right\} \quad (12)$$

These values come from the observation of a lifted multi-link object like a person.

The solution of the static problem can be obtained by substituting in (3) by $\ddot{q}(t) = \dot{q}(t) = 0$, which represents the equilibrium conditions. Therefore (3) becomes:

$$G(q) = B(q, l) u \quad (13)$$

$$\begin{bmatrix} 0 \\ (m_1 + m_2 + m_3)g \\ (m_1 L_1)g \cos \theta_1 \\ (m_2 L_{2K} + m_3 L_2)g \cos \theta_2 \\ (m_3 L_3)g \cos \theta_3 \end{bmatrix} = \begin{bmatrix} F_{1N} \sin \theta_1 - F_{2N} \sin \theta_2 - F_{3N} \sin \theta_3 \\ -F_{1N} \cos \theta_1 + F_{2N} \cos \theta_2 + F_{3N} \cos \theta_3 \\ -F_{1N} * l_1 \\ F_{2N} * l_2 \\ F_{3N} * l_3 \end{bmatrix}$$

This indicates that the object is balanced under both the gravitational and the interaction forces.

To obtain $F_{1N}, F_{2N}, F_{3N}, l_1, l_2$, and l_3 , a group of nonlinear equations are solved including (11) and:

$$\begin{aligned} (m_1 L_1)g \cos \theta_1 &= -F_{1N} * l_1 \\ (m_2 L_{2K} + m_3 L_2)g \cos \theta_2 &= F_{2N} * l_2 \end{aligned} \quad (14)$$

$$\theta_3 = \tan^{-1} \left(\frac{(F_{1N} \sin \theta_1) - (F_{2N} \sin \theta_2)}{(m_1 + m_2 + m_3)g + (F_{1N} \cos \theta_1) - (F_{2N} \cos \theta_2)} \right) \quad (15)$$

$$\begin{aligned} F_{1N} \sin \theta_1 - F_{2N} \sin \theta_2 - F_{3N} \sin \theta_3 &= 0 \\ (m_3 L_3)g \cos \theta_3 &= F_{3N} * l_3 \end{aligned} \quad (16)$$

Figure 4 shows a flow diagram of the algorithm that is proposed to solve the nonlinear equations demonstrated above. The algorithm is initialized by defining the ranges of θ_1 and θ_2 based on (12). The target is to obtain θ_3 that satisfies: the static equilibrium, (13), and the kinematic constraint, (11).

Regarding the constraint (11), l_1 and l_2 are firstly initialized by assuming that there is no radial deformation of the robot arm-1, and then (11) is solved numerically to obtain the actual lengths in the presence of the radial deformation. L_{1T} and L_{2T} are the total lengths of link-1 and link-2 respectively. l_1 and l_2 are not permissible to exceed L_{1T} and L_{2T} . The conditions $\delta_1 > 0$ and $\delta_2 > 0$ are included to guarantee that arm-1 is in contact with the links-1, 2, and they are given by:

$$\delta_i = F_{iN}/k_i \quad (17)$$

IV. EFFECT OF THE STATIC FRICTION

In this section, the static friction at the contacts between the object and the arms is considered. The magnitude and direction of the tangential force at a contact is modeled as [10]:

$$F_{iT} = \begin{cases} \in [-\mu_s F_{iN}, \mu_s F_{iN}] & v_i = 0 \\ = \mu_D F_{iN} \operatorname{sgn}(v_i) & v_i \neq 0 \end{cases} \quad (18)$$

where μ_s and μ_D are the static and the dynamic friction coefficients. For the static condition, $v_i = 0$, the magnitude and direction of F_{iT} change from $-\mu_s F_{iN}$ to $\mu_s F_{iN}$. Here, we only discuss the effect of changing the direction of F_{iT} . Since $i = 3$, there are eight cases for all the possible directions of the tangential forces F_{iT} illustrated by figure 6 in next page with a symbol for each case.

By not neglecting F_{iT} one can obtain a new relation of θ_3 given by:

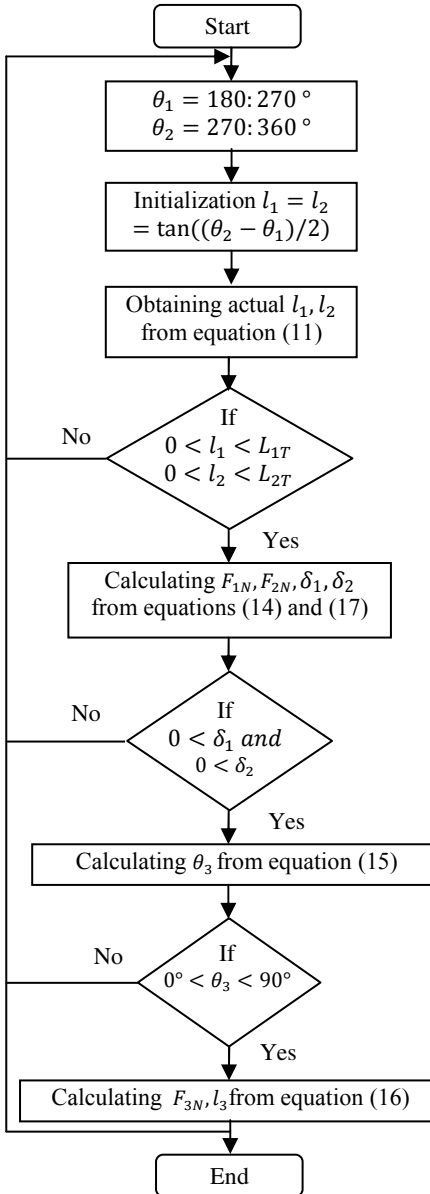


Fig. 4. Flow chart of the system static analysis

$$\theta_3 = \tan^{-1} \left(\frac{\mu_3 + \frac{F_{1x} + F_{2x}}{\sum m_i g - F_{1y} - F_{2y}}}{1 - \frac{F_{1x} + F_{2x}}{\sum m_i g - F_{1y} - F_{2y}} \mu_3} \right) \quad (19)$$

where $F_{1x}, F_{1y}, F_{2x}, F_{2y}$ are defined from (6) and μ_3 is the static friction coefficient between arm-2 and link-3 which equals $\pm \mu_s$. F_{1T} and F_{2T} are given by:

$$F_{1T} = \mu_1 F_{1N}, F_{2T} = \mu_2 F_{2N} \quad (20)$$

μ_1, μ_2 are the static friction coefficients between arm-1 and links-1 & 2 respectively, and equal $\pm \mu_s$.

The same procedure is followed to solve the static analysis of the system as in the frictionless case except in the calculation of θ_3 solved by (20). An extra constraint $\delta_3 > 0$ is added; this guarantees that link-3 and arm-2 are both in contact.

V. SIMULATION RESULTS

A. The Condition of Frictionless Contact

The system parameters applied for simulation are shown in Table I. Figure 5 illustrates the contour lines of θ_3 that define the relations between θ_1 and θ_2 to keep the system at equilibrium for all configurations of link-1 and link-2. Figure 7 illustrates the changes of θ_3 when the difference between θ_1 and θ_2 is increased. For each configuration of θ_1 and θ_2 , there is only one value of θ_3 that delivers the system to an equilibrium state, within the range of θ_2 , less than 320°. There is also a discontinuity in the contour lines of θ_3 which occurs when the difference between θ_1 and θ_2 is around 90° from (11).

TABLE I
PHYSICAL PARAMETERS OF THE SYSTEM

| Symbol | $i = 1$ | $i = 2$ | $i = 3$ |
|--------------|---------|---------|---------|
| m_i [Kg] | 7 | 20 | 43 |
| L_i [m] | 0.25 | 0.24 | 0.35 |
| L_{iT} [m] | 0.45 | 0.42 | 0.88 |
| r_i [m] | 0.1 | 0.1 | 0.1 |
| k_i [N/m] | 10^5 | 10^5 | 10^5 |
| μ_s | 0.9 | 0.9 | 0.9 |

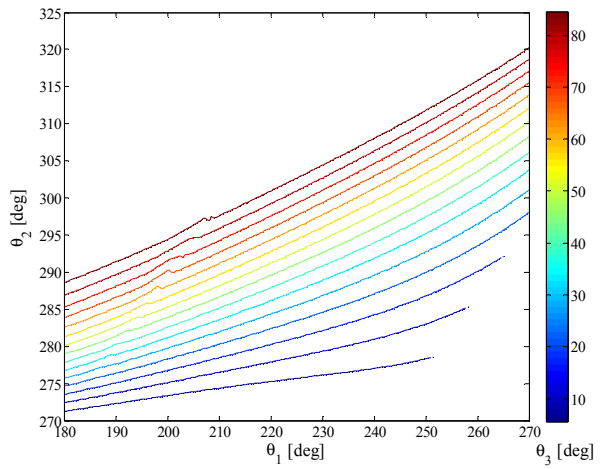


Fig. 5. Change of θ_3 with θ_1 and θ_2

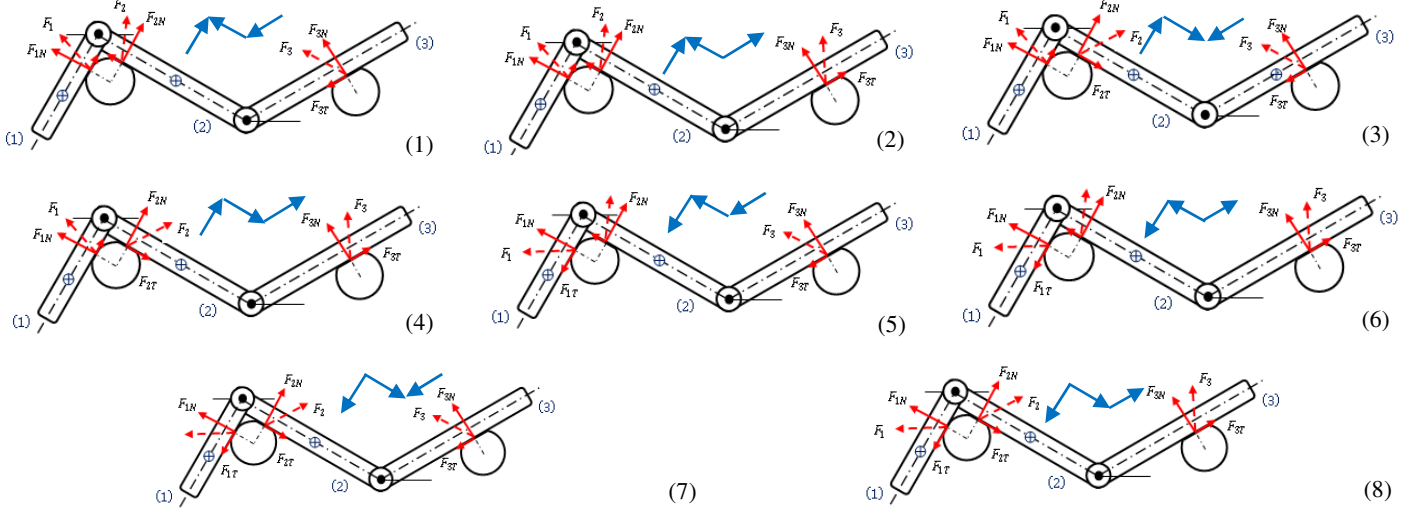


Fig. 6. Different directions of the tangential forces F_{iT}

Figures 8 and 9 shows the contour lines of the change of F_{1N} and l_1 with θ_1 and θ_2 . The same will be for F_{2N} and l_2 . The behaviors of F_{1N} and l_1 are inversely proportional to each other. F_{1N} increases as the angle between the links-1 & 2 is decreasing. Regarding F_{3N} it is better to express it in terms of $(\theta_2 - \theta_1)$ and θ_3 , see figure 10.

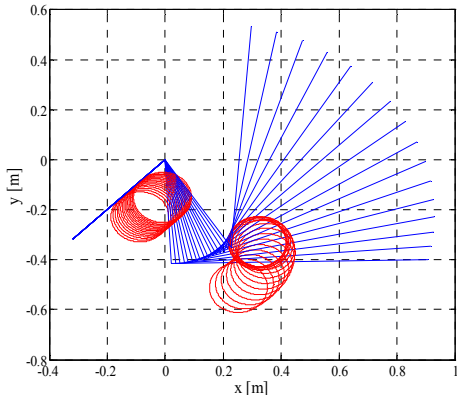


Fig. 7. Change of θ_3 with constant θ_1 and increased θ_2

The minimum F_{3N} is obtained at nearly about $(\theta_2 - \theta_1) \approx 90^\circ$ & 45° , and θ_3 is less than 20° and around 70° respectively. l_3 will be inversely proportional to F_{3N} .

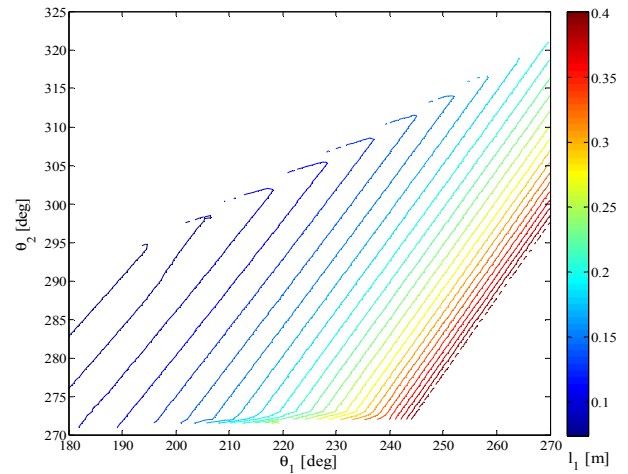


Fig. 9. Change of l_1 with θ_1 and θ_2

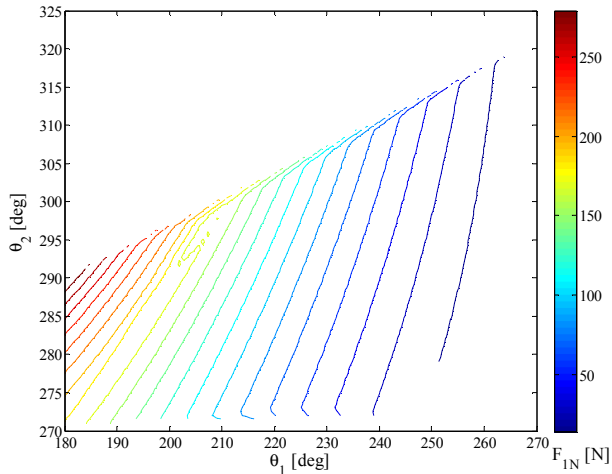


Fig. 8. Change of F_{1N} with θ_1 and θ_2

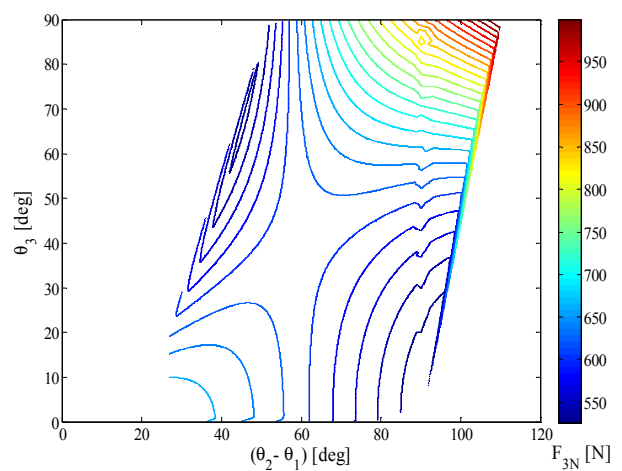


Fig. 10. Change of F_{3N} with $(\theta_2 - \theta_1)$ and θ_3

B. The Condition of Frictional Contact

The effect of changing the direction of the static frictional forces appears in terms of changing θ_3 and hence F_{3N} and l_3 , for a specified configuration of θ_1 and θ_2 . F_{1N}, F_{2N}, l_1 , and l_2 are the same as the frictionless case. Figure 11 shows different equilibrium values of θ_3 for a certain θ_1 and θ_2 . Figure 12 shows the contour lines of θ_3 with θ_1 and θ_2 for only case (4) of the directions of F_{iT} . Not all the cases are included because of the limited space. One can conclude the followings:

- 1) θ_3 increases with increasing the difference ($\theta_2 - \theta_1$)
- 2) The working range of θ_2 decreases compared to the frictionless case and it is different for each case
- 3) The minimum range of θ_3 is for the cases (1) and (5) where the directions of F_{2T} and F_{3T} are the same.

VI. CONCLUSIONS

The dynamic modeling of a three-rigid link object manipulated by two cooperative arms has been derived. This could be considered as an initial step towards the more complicated problem of multi elastic deformable link-object manipulation. Kinematic constraint of link-1 and link-2 with arm-1 has been considered in order to insure that arm and the two links are in contact all the time. The static analysis of the system has been performed for the friction and frictionless conditions to obtain the interaction forces and their locations for each configuration of the links' angular positions. An algorithm has been proposed to solve the analysis problem.

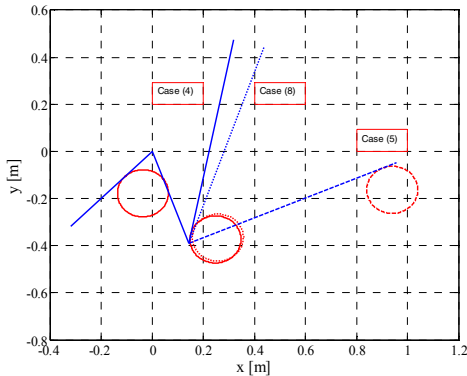


Fig. 11. Change of θ_3 for a certain θ_1 and θ_2

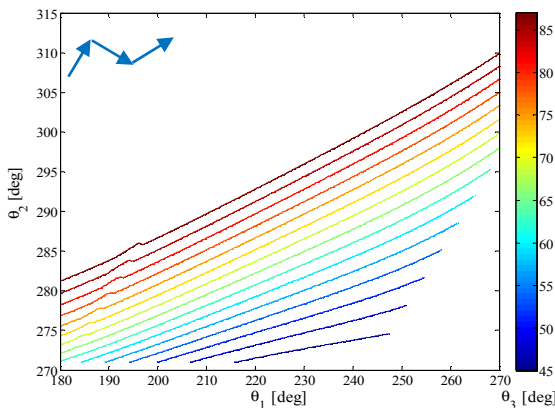


Fig. 12. Change of θ_3 with θ_1 and θ_2 for case (4)

It is sufficient to know the angles of link-1 and link-2 to determine the orientation of link-3 and the interaction forces as well as their locations to keep the system at an equilibrium position. The effect of the direction of the static frictional forces has been explored as well. The direction of the static frictional forces affects the angular position of link-3 required for equilibrium for a certain configuration of link-1 and link-2. Its higher and lower values are obtained when all the friction forces are in the same direction. Compared to the frictional case the range of the angular position of link-3 required for equilibrium is decreased. The effect of changing the value of the static friction coefficient, the design of a controller for the system with considering the dynamics of the arm in progress and its results will be reported in the future.

ACKNOWLEDGMENT

The first author is supported by a scholarship from the Mission Department, Ministry of Higher Education of the Government of Egypt which is gratefully acknowledged.

REFERENCES

- [1] Mukai, T.; Hirano, S.; Nakashima, H.; Kato, Y.; Sakaida, Y.; Guo, S.; Hosoe, S., "Development of a nursing-care assistant robot RIBA that can lift a human in its arms," *IEEE/RSJ International Conference on Intelligent Robots and Systems (IROS)*, 2010, vol., no., pp.5996,6001, 18-22 Oct. 2010.
- [2] Mukai, T.; Hirano, S.; Yoshida, M.; Nakashima, H.; Guo, S.; Hayakawa, Y., "Whole-body contact manipulation using tactile information for the nursing-care assistant robot RIBA," *IEEE/RSJ International Conference on Intelligent Robots and Systems (IROS)*, 2011, vol., no., pp.2445,2451, 25-30 Sept. 2011
- [3] Mason, Matthew T.; Lynch, K.M., "Dynamic manipulation," *IEEE/RSJ International Conference on Intelligent Robots and Systems, IROS '93*, vol.1, no., pp.152,159 vol.1, 26-30 Jul 1993
- [4] Asano, F.; Saitoh, Y.; Watanabe, K.; Zhi-Wei Luo; Yamakita, M., "On dynamic whole body manipulation," *IEEE International Symposium on Computational Intelligence in Robotics and Automation, 2003*, vol.3, no., pp.1201,1206 vol.3, 16-20 July 2003
- [5] Lynch, K., and Mason, M., "Dynamic nonprehensile manipulation: controllability, planning, and experiments," *International Journal of Robotics Research*, vol. 18, No. 1, pp. 64-92, 1999.
- [6] Beigzadeh, B.; Ahmadabadi, M.N.; Meghdari, A., "Two Dimensional Dynamic Manipulation of a Disc Using Two Manipulators," *IEEE International Conference on Mechatronics and Automation, Proceedings of the 2006*, vol., no., pp.1191,1196, 25-28 June 2006
- [7] Mori, W.; Ueda, J.; Ogasawara, T., "1-DOF dynamic pitching robot that independently controls velocity, Angular velocity, and direction of a ball: Contact models and motion planning," *IEEE International Conference on Robotics and Automation, 2009. ICRA '09.*, vol., no., pp.1655,1661, 12-17 May 2009
- [8] Higashimori, M.; Utsumi, K.; Omoto, Yasutaka; Kaneko, M., "Dynamic Manipulation Inspired by the Handling of a Pizza Peel," *IEEE Transactions on Robotics*, , vol.25, no.4, pp.829,838, Aug. 2009
- [9] Onishi, M.; Odashima, T.; Zhiwei Luo, "Emergent cooperative manipulation of a multi-linked object," *Annual Conference SICE 2003*, vol.3, no., pp.3049,3052, 4-6 Aug. 2003
- [10] Zyada, Z.; Hayakawa, Y., and Hosoe, S., "Kinematic Analysis of a Two-Link Object for Whole Arm Manipulation," *International Conference on Signal Processing, Robotics and Automation, ISPRA10*, University of Cambridge, UK, February 20-22, 2009.
- [11] Zyada, Z.; Hayakawa, Y.; Hosoe, S., "Model-based control for nonprehensile manipulation of a two-rigid-link object by two cooperative arms," *IEEE International Conference on Robotics and Biomimetics (ROBIO)*, 2010, vol., no., pp.472,477, 14-18 Dec. 2010
- [12] Zyada, Z.; Hayakawa, Y.; and Hosoe, S., "Fuzzy Nonprehensile Manipulation Control of a Two-Rigid-Link Object by Two Cooperative Arms," *18th World Congress of the International Federation of Automatic Control, IFAC*, vol. 18, pp.14614, 14621, Sep. 2011.